Organic & Biomolecular Chemistry

Accepted Manuscript

ROYAL SOCIETY OF CHEMISTRY

www.rsc.org/obc

Journal Name

RSCPublishing

ARTICLE

A novel chemosensor with visible light excitability for sensing Zn^{2+} in physiological medium and in HeLa cells

Cite this: DOI: 10.1039/x0xx00000x

Barun Kumar Datta,[a] Durairaj Thiyagarajan,[b] Soham Samanta,[a] Aiyagari Ramesh,*[b] and Gopal Das*[a]

Received ooth January 2012,
Accepted ooth January 2012

DOI: 10.1039/x0xx00000x

www.rsc.org/

In the present study a novel imine-hydrazone based fluorescent chemosensor (**L_1**) for efficient and selective sensing of Zn^{2+} over other biologically important metal ions in physiological conditions is reported. Enhancement in fluorescence emission intensity of the developed probe with a red shift of ~25 nm was observed with Zn^{2+}, whereas other metal ions failed to reveal any significant change in the emission spectra. Interestingly, the receptor functioned in completely physiological condition (99.7% HEPPES buffer) and has visible light excitability. Sensing of Zn^{2+} was investigated in detail through absorption spectroscopy, emission spectroscopy, DFT calculation, ^{1}H-NMR titration experiment and ESI-MS experiment. Association constant between **L_1** and Zn^{2+} was found to be 5.58×10^5 M^{-1}. The receptor could detect as low as 69 ppb Zn^{2+}. Sensing of Zn^{2+} is proposed through switch-on of intramolecular charge transfer (ICT) and chelation enhanced fluorescence (CHEF) process after the introduction of Zn^{2+} to the free ligand. The developed receptor was non-toxic and rendered intracellular sensing of Zn^{2+} in HeLa cells through fluorescence imaging studies.

Introduction

Detection and imaging of biologically relevant target molecules through fluorescence in living systems has emerged as an area of intense interest in the chemistry-biology interface owing to its significant biomedical implications.[1] Among many of the biologically important metal ions, Zn(II) is known to play crucial roles in the activity of various enzymes and also a key component of some transcription factors, gene expression, apoptosis, neurotransmission and so forth.[2] Perturbations in zinc homeostasis is of high concern resulting in disorders such as impaired cognition, immune dysfunction, type 2 diabetes mellitus (T2DM), Alzheimer's disease, epilepsy, ischemic stroke, and age-related macular degeneration (AMD), infantile diarrhoea.[3] Being a harmful pollutant, zinc is also important for environmental safety.[4]

Imaging of intracellular Zn^{2+} with fluorescent chemosensors has been established as an efficient tool to provide chronological–spatial evidence on Zn^{2+} homeostasis in live cells.[5] In general, most fluorogenic chemosensors depend on the change of emission intensity (quenching, enhancement, or ratiometric) of the chromophore units which acts as signalling unit for the sensing ability.[6] Even though sensing of analytes in solution can be correlated with the systematic variations in emission intensity but the detection of analytes in cells is fraught with the challenge of specific sensing in a complex milieu. For example, during imaging cells using fluorescence microscopy, quenching may occur due to the photobleaching[7] and/or aggregation[8] to several degrees in different cellular environments. Furthermore, lives cell imaging with a probe within biological cells may result in heterogeneous labelling of the sensor, which can lead to varying emission intensities at different spatial positions.[9] The aforementioned anomaly present great challenge towards analysing signal change due to the recognition of the analytes with those arising from variations in probe concentration within cells. Therefore, it is significant to design new sensors which undergo profound spectroscopic changes like spectral shifts, upon binding with the analyte like Zn^{2+}. Fluorescent probes are designed on the basis of inter charge transfer (ICT),[10] photoinduced electron transfer (PET),[11] chelation-enhanced fluorescence (CHEF),[12] metal–ligand charge transfer (MLCT),[13] excimer/exciplex formation,[14] imine isomerization,[15] intermolecular hydrogen bonding,[16,14e] excited-state intramolecular proton transfer,[17] displacement approach,[18,23g,23h] and fluorescence resonance energy transfer.[19] CHEF is an important process by which fluorescent probes detect analytes.[12] When the CHEF process is in switch-on condition, the conjugation increases drastically which leads to enhancement in the emission and also a red shift is expected. So, the fluorophore probe senses a metal ion with

enhancement in the emission intensity accompanied by a red shift.

Considering the physiological and biomedical significance of zinc, there is an overriding interest in the development of selective and sensitive zinc sensors. Zn^{2+} ion does not respond to common analytical techniques like Mossbauer, NMR, and electron paramagnetic resonance (EPR) as compared to other transition metal ions like Fe^{2+}, Mn^{2+} and Cu^{2+}. Thus it is difficult to trace zinc ion in highly complex biological systems. So far, a number of fluorescent chemosensors for selective detection of Zn(II)- have been reported with some success in biological applications,[20] but most of the reported fluorescent as well as colorimetric sensors for Zn^{2+} work in either pure organic or mixture organic-aqueous solutions.[21] This restricts their applications in a physiological environment. Hence there is a critical demand to develop fluorescent probe for Zn^{2+} that are based on easy synthesis, render visible light excitation, exhibit large red-shift in emission for Zn^{2+} sensing, and their sensing capability is immune from any pH interference in the physiological range.

In our continuous endeavour of sensing various analytes[22], herein we report the synthesis, characterization and sensing behaviour of a novel fluorescent chemosensor towards Zn^{2+} with visible light excitability and the ability to sense the metal in completely physiological condition. The recognition of Zn^{2+} by our receptor $\mathbf{L_1}$ has been investigated by absorption spectroscopy, emission spectroscopy, DFT calculation, ESI-MS experiment and ^{1}H-NMR titration. Detection of intracellular zinc in live HeLa cells through fluorescence imaging is also demonstrated in the study.

Experimental Section

General Information and Materials

All the materials used for synthesis were purchased from commercial suppliers and used without further purification. 2, 6-Diformyl-4-methylphenol (DFMP) was prepared by modification of the literature method.[23] Absorption spectra were recorded on a Perkin-Elmer Lamda-750 UV−vis spectrophotometer using 10 mm path length quartz cuvettes in the range of 250−700 nm wavelength. Fluorescence measurements were conducted on a Fluoromax-4 spectrofluorometer using 10 mm path length quartz cuvettes with a slit width of 5 nm at 298 K. All the mass spectra were obtained using Agilent Technologies 6520 Accurate mass spectrometer. NMR spectra were recorded either on a Varian FT-400 MHz instrument or on a Bruker 600MHz instrument. The chemical shifts were recorded in parts per million (ppm) on the scale. The following abbreviations are used to describe spin multiplicities in ^{1}H NMR spectra: s = singlet; d = doublet; t = triplet; m = multiplet.

Synthesis of the Receptor

The synthetic routes of the two compounds $\mathbf{L_1}$ and $\mathbf{L_2}$ are depicted in scheme 1.

Synthesis of picolinichydrazide

Picolinic acid was dissolved in ethanol and in ice cold condition thionyl chloride was added drop wise over a period of 30 min with constant stirring. After 1 hour stirring, the hazy mixture was refluxed overnight. After evaporation of the solvent, water was added and the pH was adjusted to 8.0 by the addition of sodium bicarbonate. Subsequently the mixture was extracted with ethyl acetate (3x50 ml). The organic layer was dried over sodium sulphate and evaporation of the solvent gave the ethyl ester of picolinic acid as a colourless liquid. This ester was used without further purification. This ester was then treated with excess hydrazine monohydrate in

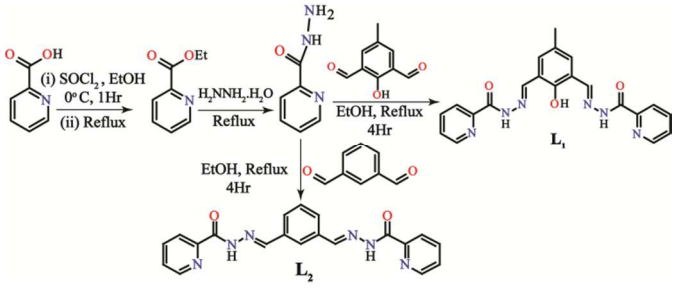

Scheme 1. Synthesis of $\mathbf{L_1}$ and $\mathbf{L_2}$.

ethanol. The mixture was heated to reflux for overnight. After evaporation of the solvent and the excess hydrazine under reduced pressure, a white solid was obtained, which was dried in vacuum and was used in the next step without further purification.

Synthesis of $\mathbf{L_1}$

2,6-Diformyl-4-methylphenol (1 mmol) was dissolved in ethanol. Picolonic hydrazide (2 mmol) was added to the above solution and the mixture was refluxed for 4 hours to give a yellow crystalline product. Yield 72%. ^{1}H NMR [400 MHz, DMSO-d_6, δ (ppm)]: 11.47 (2H, s), 11.26 (1H, s), 7.84 (2H, s), 7.67 (2H, d, J = 4.4 Hz), 7.08 (2H, d, J = 7.6 Hz), 7.01 (2H, t, J= 7.8 Hz), 6.62 (2H, t, J = 5.8 Hz), 6.48 (2H, s), 1.25 (3H, s). ^{13}C NMR [100 MHz, DMSO-d_6, δ (ppm)]: 160.8, 155.0, 149.3, 148.8, 147.8, 138.2, 130.8, 128.4, 127.3, 122.9, 120.1, 20.0. ESI-MS (positive mode, *m/z*) Calculated for $C_{21}H_{19}N_6O_3$ [$\mathbf{L_1}$ +H] = 403.1519, Found 403.1546.

Synthesis of $\mathbf{L_2}$

Isophthaldehyde (1 mmol) was dissolved in ethanol, picolonic hydrazide (2 mmol) was added to the above solution and the mixture was refluxed for 4 hours to give a white crystalline product. Yield 75%. ^{1}H NMR [400 MHz, $CDCl_3$, δ (ppm)]: 11.09 (2H, s), 8.60 (2H, d, J=8 Hz), 8.32 (4H, d, J = 8.4 Hz), 8.17 (1H, s), 7.94-7.89 (4H, m, J = 3.6 Hz), 7.52-7.47 (3H, s). ^{13}C NMR [100 MHz, $CDCl_3$, $SiMe_4$, δ (ppm)]: 160.4, 149.2, 148.3, 148.1, 137.8, 134.4, 129.6, 129.3, 127.7, 127.0, 123.1. ESI-MS (positive mode, *m/z*) Calculated for $C_{20}H_{17}N_6O_2$ [$\mathbf{L_2}$ +H] = 373.1413, Found 373.1426.

UV−visible and Fluorescence Spectroscopic Studies

Stock solutions of various ions (1×10^{-3} molL^{-1}) were prepared in deionized water. Perchlorate, chloride or nitrate salts of metal ions were used to prepare metal stock solutions. A stock solution of $\mathbf{L_1}$ (1×10^{-3} molL^{-1}) was prepared in DMSO. The solution of $\mathbf{L_1}$ was then diluted to 1×10^{-6} molL^{-1} with aqueous HEPES buffer (1 mM, pH 7.4). All the spectroscopic experiments were performed in aqueous HEPES buffer medium (1 mM, pH 7.4) containing 0.33% of DMSO. In titration experiments, a solution of $\mathbf{L_1}$ (1×10^{-6} molL^{-1}) was filled in a quartz optical cell of 1.0 cm optical path length, and the ion stock solutions were added gradually to achieve a concentration of 1×10^{-5} molL^{-1}. In selectivity experiments, the test samples were prepared by interacting appropriate amounts of the cations stock into 2 mL of $\mathbf{L_1}$ solution (2×10^{-5} molL^{-1}). For all the samples, the spectra were recorded following 1 min of the addition of the ions. For fluorescence measurements, excitation wavelength was set at 470 nm and emission was recorded from 480 nm to 700 nm. The selective binding of $\mathbf{L_1}$ with Zn^{2+} among all other metal ions was also studied by fluorescence emission spectroscopy of the solution of $\mathbf{L_1}$ (10.0×10^{-6} molL^{-1}) in the absence and presence of an excess (10 eq.) of each of the metal ions in mixed solvent.

Evaluation of the Apparent Binding Constant for the Formation of $\mathbf{L_1}\cdot2Zn^{2+}$

A stock solution of $Zn(ClO_4)_2$, having a concentration of 0.5×10^{-3} molL^{-1}, in an aqueous HEPES buffer (pH 7.4) solution was used. Receptor $\mathbf{L_1}$ with an effective concentration of 10.0×10^{-6} molL^{-1} in the aforementioned HEPES buffer medium was used for the emission titration studies. The effective Zn^{2+} concentration was varied between 0 and 10×10^{-5} molL^{-1} for this titration. The solution pH was adjusted to 7.4 using an aqueous HEPES buffer solution having an effective concentration of 1.0 mM.

The apparent binding constant for the formation of the respective complexes were evaluated using the Benesi−Hildebrand (B−H) plot (equation 1).[24]

$$1/(I-I_0) = 1/\{K(I_{max}-I_0)C\} + 1/(I_{max}-I_0) \quad (1)$$

I_0 is the emission intensity of $\mathbf{L_1}$ at λ = 550 nm, I is the observed emission intensity at that particular wavelength in the presence of a certain concentration of the metal ion (C), I_{max} is the maximum emission intensity value that was obtained at λ = 550 nm during titration with varying metal ion concentration, K is the apparent binding constant (M^{-1}) and was determined from the slope of the linear plot, and C is the concentration of the Zn^{2+} ion added during titration studies.

Detection Limit for Zn^{2+} ion

The detection limit was calculated on the basis of the fluorescence titration. The fluorescence emission spectrum of $\mathbf{L_1}$ was measured 10 times, and the standard deviation of blank measurement was achieved. To gain the slope, the ratio of the emission intensity at 560 nm was plotted as a concentration of Zn^{2+}. The detection limit was calculated using the following equation

$$\text{Detection limit} = 3\sigma/k \quad (2)$$

where σ is the standard deviation of blank measurement, and k is the slope between the ratio of emission intensity versus $[Zn^{2+}]$.

Detection of Zn^{2+} in HeLa Cells by fluorescence microscope analysis

HeLa cells (human cervical carcinoma cells) were initially cultured in a 25 cm^2 tissue culture flask containing DMEM medium supplemented with 10% FBS, penicillin (100 µg/mL) and streptomycin (100 µg/mL) in a CO_2 incubator. Prior to cell imaging studies, HeLa cells were seeded into a 6 well plate and grown in DMEM medium at 37◦C till 80% confluency in a CO_2 incubator. Subsequently, the cells were washed thrice with sterile phosphate buffered saline (PBS), incubated with 25 µM $\mathbf{L_1}$ in DMEM at 37◦C for 1 hr in a CO_2 incubator and their images were acquired using a fluorescence microscope (Eclipse Ti–U, Nikon, USA) with a filter that allowed green light emission. The cells were further washed with sterile PBS in order to remove excess $\mathbf{L_1}$, and then incubated for 1 hr with 50 µM $Zn(ClO_4)_2$ made in sterile PBS. The images of the cells were again acquired with a fluorescence microscope as mentioned earlier.

Results and Discussion

Sensing of Zn^{2+}

ABSORPTION SPECTROSCOPIC STUDIES

All the spectroscopic studies were performed in HEPES buffer medium (1 mM, pH=7.4) containing 0.33% of DMSO.

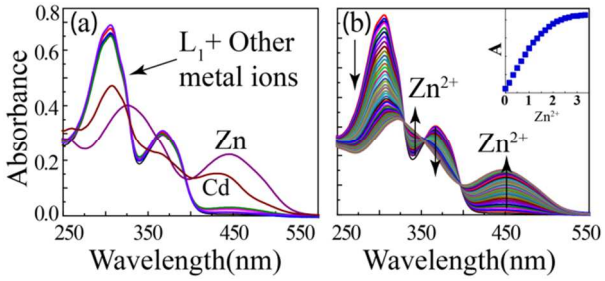

Fig.1: Changes in absorption spectroscopy of $\mathbf{L_1}$ (25 µM) with (a) various metal ions (10 eq.) and (b) with incremental addition of Zn^{2+} (0 µM – 60 µM). Inset: Plot of absorbance at 450 nm vs $[Zn^{2+}]$.

The ligand $\mathbf{L_1}$ exhibited two characteristic absorption peaks at 305 nm (ε= 4x10^4 M^{-1}cm^{-1}) and 367 nm (ε= 1.8x10^4 M^{-1}cm^{-1}), which may be attributed to the π−π* transitions and the long conjugation present in the free ligand system. Upon addition of 10 equivalent of different metal ions (Na^+, K^+, Mg^{2+}, Ca^{2+}, Co^{2+}, Ni^{2+}, Cu^{2+}, Cd^{2+}, Ag^+, Pb^{2+}, Hg^{2+}, Al^{3+}, Cr^{3+}, Fe^{3+}, Zn^{2+}) Zn^{2+} promoted a prominent change in the absorption spectra of $\mathbf{L_1}$ (Figure 1a). Amongst other metals, only Cd^{2+} caused a

nominal change in the absorption spectra of **L_1.** However, this change was distinctly less in magnitude as compared to the change observed with Zn^{2+} (Fig. 1a). Upon the addition of Zn^{2+} ion (10 eq.), the absorption peak at 305 nm (ε= 1.8x10^4 M^{-1}cm^{-1}) decreased and shifted to 326 nm and a new peak emerged at 450 nm (ε= 0.98x10^4 M^{-1}cm^{-1}). On the other hand, with the addition of Cd^{2+} the absorption at 305 nm (ε= 3x10^4 M^{-1}cm^{-1}) decreased, akin to that observed with Zn^{2+}, while a new peak appeared at 436 nm (ε= 0.24x10^4 M^{-1}cm^{-1}). Incremental addition of Zn^{2+} to **L_1** resulted in three isosbestic points at 329 nm, 352 nm and 396 nm indicating the transition of the free ligand into metal complex (Figure 1b). A visual colour change was observed during the above process from colourless to yellow (Fig. S13). From the absorption titration experiment it was also witnessed that change in the absorption spectra became minimum after the addition of two equivalent of metal ion (Fig. 1b inset) which suggested a 1:2 binding stoichiometry between **L_1** and Zn^{2+}. Essentially, absorption spectrum indicated that the receptor exhibited high selectivity towards Zn^{2+} with a marginal response to Cd^{2+}.

Fluorescence spectroscopic studies of L_1 in presence of metal ions

With visible light excitability, when the receptor (**L_1**) was excited at 470 nm, a weak emission peak was observed at ~530 nm. A set of different metal ions (Na^+, K^+, Mg^{2+}, Ca^{2+}, Co^{2+}, Ni^{2+}, Cu^{2+}, Cd^{2+}, Ag^+, Pb^{2+}, Hg^{2+}, Al^{3+}, Cr^{3+}, Fe^{3+}, Zn^{2+}) were used to ascertain the selectivity of **L_1**. Interestingly only Zn^{2+} caused a drastic enhancement in the emission intensity of **L_1** with a prominent peak obtained at 555 nm while Cd^{2+} causes a very small enhancement in the emission intensity (Fig. 2a). This observation clearly demonstrated high selectivity of **L_1** towards Zn^{2+} over other metal ions including Cd^{2+}. During titration with Zn^{2+}, **L_1** displayed a linear enhancement in the emission intensity of the free ligand with a progressive red shift (Figure 2b). After the addition of two equivalent of Zn^{2+} ion the change in the emission spectra

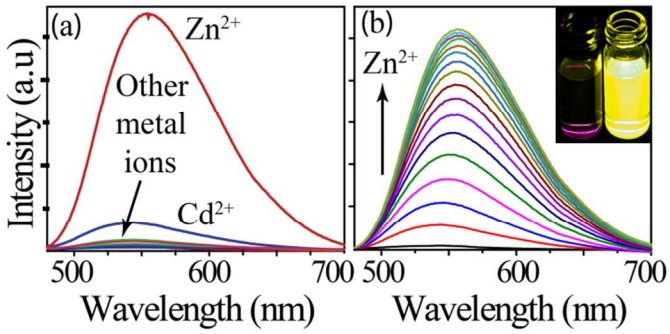

Fig.2: Changes in emission spectra of **L_1** (25 μM) in presence of (a) various metal ions (10 eq.) and (b) with incremental addition of Zn^{2+} (0 μM - 60μM). Inset: Change in colour change under UV lamp (λ_{em}= 365nm) upon addition of Zn^{2+} to **L_1**.

became minimal supporting the result obtained from UV-Vis experiment (Fig. 2b). Fluorescence quantum yields of the Zn^{2+} complex was calculated to be 18-times higher than that of the probe alone (0.16 and 0.009, respectively). A change in the fluorescence emission from colourless to yellow was observed under UV-lamp after the addition of Zn^{2+} to the receptor solution (Fig. 2b inset). Careful analysis of Job's plot (Fig. S11) obtained from the fluorescence titration experiment established a 1:2 binding stoichiometry between **L_1** and Zn^{2+}. The association constant and detection limit of **L_1** for Zn^{2+} were calculated to be 5.58 ×10^5 M^{-1} (Fig. S12) and approximately 69 ppb respectively.

The amplification of fluorescence intensity of the receptor, **L_1** by Zn^{2+} was also confirmed through screening with competing metal cations of interest (Fig. 3). Except for Zn^{2+}, only Cd^{2+} among the verified cations triggered the emission enhancement, but it was negligible as compared to that of Zn^{2+}. It is to be noted that even highly abundant intracellular alkali metal ions (Na^+, K^+) and alkaline earth metal ions (Mg^{2+}, Ca^{2+}) did not affect the emission spectra of **L_1** even in the presence of excess amount. The effect of different counter anions of zinc salt was also investigated in the same condition using different zinc salts like Zn $(ClO_4)_2$, Zn $(OAc)_2$, Zn $(NO_3)_2$, $ZnCl_2$, $ZnBr_2$ and $ZnSO_4$. From the experiment it was found that the counter anions of zinc did not influence the recognition process of Zn^{2+} by **L_1**.

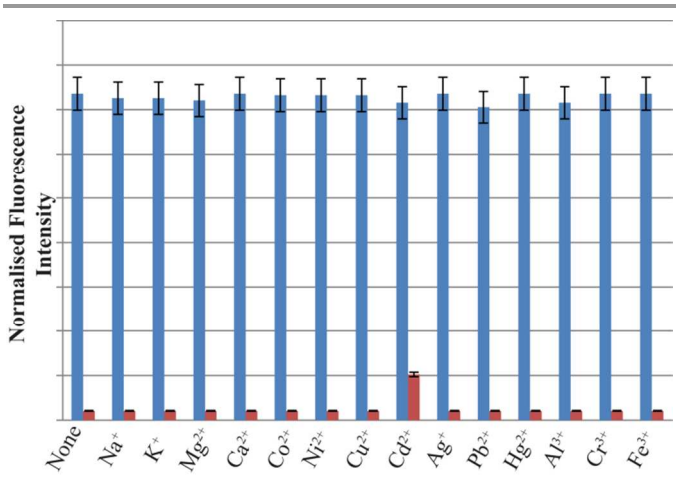

Fig.3: Normalized fluorescence responses of **L_1** (10 μM) at 550 nm in presence of various cations in mixed solvent. The red bars represent the emission intensities of **L_1** in the presence of cations of interest (5.0 eq.). The blue bars represent the change of the emission upon subsequent addition of Zn^{2+} to the above solution. Display error bars with 5% values.

pH Dependent study

The fluorescence property of the receptor, **L_1** was checked at different pH. At lower pH (2-6), the receptor displayed blue fluorescence whereas at higher pH (9 and above) the receptor exhibited a yellow fluorescence with lower intensity. Possibly at lower pH, protonation or hydrolysis of the imine bond may have resulted in a blue fluorescence. On the other hand, at higher pH deprotonation of the hydroxyl group perhaps leads to a weak yellow fluorescence. Interestingly, it was observed that the ligand has stable fluorescence within the pH range of 6.5-9.0. This observation suggested that the ligand could render pH-independent fluorescence measurement in physiological

microenvironment. The high selectivity of $\mathbf{L_1}$ towards Zn^{2+} over other biologically important metal ions, its sensing capability in physiological condition and a lower detection limit enhances the analytical merit of the developed receptor ($\mathbf{L_1}$) for the recognition of intracellular Zn^{2+}.

^{1}H NMR Titration

We were unsuccessful to get a single crystal of the Zn^{2+} complex of $\mathbf{L_1}$ suitable for X-ray diffraction even after several attempts. Therefore, in order to understand the mode of interaction between $\mathbf{L_1}$ and Zn^{2+} or the structural changes in $\mathbf{L_1}$ after interacting with Zn^{2+}, we acquired ^{1}H-NMR data. ^{1}H-NMR titration of the receptor, $\mathbf{L_1}$ with $Zn(ClO_4)_2$ was performed in DMSO-d_6. During ^{1}H-NMR titration of $\mathbf{L_1}$ with Zn^{2+} significant spectral changes of $\mathbf{L_1}$ were observed. Reduction in the intensity of the hydroxyl group (-OH) indicated deprotonation as a result of interaction with Zn^{2+} and after the addition of two equivalent of Zn^{2+} ion, the hydroxyl group peak was obliterated. As illustrated in Fig. S14, upfield shifts were observed in the case of the pyridyl hydrogen atoms. The Schiff base hydrogen atom and the hydrogen atoms on the DFMP ring also underwent upfield shifts whereas very little change was observed for the amide proton (-NH) as compared to the other protons within the system. Collectively ^{1}H-NMR titration strongly suggested the formation of a hydroxo bridged complex between $\mathbf{L_1}$ and Zn^{2+} resulting in the deprotonation of the hydroxyl group and the pyridyl nitrogen atom coordinating to Zn^{2+} causing shifts to the pyridyl hydrogen atoms.

ESI-MS Experiment

The binding mode between $\mathbf{L_1}$ and Zn^{2+} was also investigated through ESI-MS. A peak at 869.8240 signifies the mass of the ensemble ($\mathbf{L_1}$+2Zn+3ClO_4+CH_3CN) $C_{23}H_{21}Cl_3N_7O_{15}Zn_2$ and another peak at 403.1546 represents the mass of the free receptor. So, the result from ESI-MS experiment also supports the results obtained from the UV-Vis and emission spectroscopy.

Mechanism of Zn^{2+} Sensing

The enhancement in the fluorescence intensity of the receptor, $\mathbf{L_1}$ after interacting with Zn^{2+} may be attributed to the CHEF and ICT process. Firstly, the low fluorescence of $\mathbf{L_1}$ may be due to the free rotation of the imine (-C=N) bond. As illustrated in scheme 2, in presence of Zn^{2+}, chelation of the metal ion with the –OH group and with the two imine N-atoms ensues. Consequently, the free rotation around the imine bond gets restricted and the system becomes more rigid. Furthermore, chelation of Zn^{2+} by the hydroxide group and the Schiff base N-atoms leads to the formation a hydroxo bridged binuclear zinc complex in which the conjugation increases drastically resulting in a CHEF effect. On the other hand, due to the binding of Zn^{2+} the ICT is facilitated over the π-system. This also caused sufficient enhancement in the fluorescence. The CHEF phenomenon in conjunction with the ICT process upon interacting with Zn^{2+}, perhaps results in the enhancement the fluorescence intensity of the free receptor along with a red shift of ~25 nm. The proposed CHEF mechanism was verified by conducting control experiments with the receptor $\mathbf{L_2}$, which lacked the hydroxyl group. As anticipated, $\mathbf{L_2}$ did not show any change in its emission spectra after interaction with Zn^{2+} owing to the lack of chelation of Zn^{2+} and a CHEF effect thereof. This result strongly suggested that the di-imine moiety with the hydroxyl group at the core was essentially implicated in the Zn^{2+} sensing phenomenon.

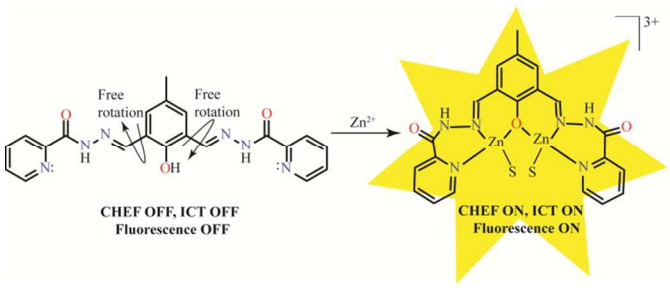

Scheme 2. Proposed mechanism of sensing.

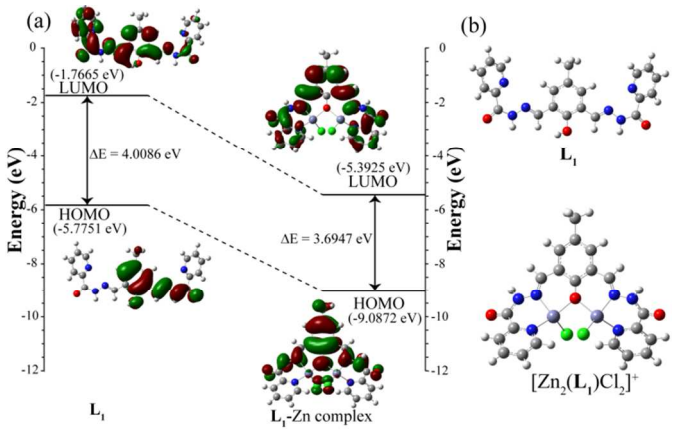

Fig. 4: (a) Energy diagrams of HOMO and LUMO orbitals of $\mathbf{L_1}$ and the $\mathbf{L_1}$–Zn complex calculated at the DFT level using a B3LYP/6-31+G(d,p) basis set. (b) Optimized structure of $\mathbf{L_1}$ and its Zn^{2+} complex.

Further, the above premise of our proposed sensing mechanism was corroborated with the theoretical calculations of $\mathbf{L_1}$ and its Zn complex. To understand the relationship between the structural changes of $\mathbf{L_1}$ and its complex with Zn^{2+} and the optical response of $\mathbf{L_1}$ to Zn^{2+}, we carried out density functional theory (DFT) calculations with the B3LYP/6-31+G(d,p) method basis set using the Gaussian 03 program. The optimized geometry along with the highest occupied molecular orbital (HOMO) and the lowest unoccupied molecular orbital (LUMO) of $\mathbf{L_1}$ and its Zn^{2+} complex are presented in Fig. 3. These HOMO and LUMO energy diagrams revealed that the energy gap for the di-nuclear Zinc complex of $\mathbf{L_1}$ (two Zinc ions are linked through the Oxo-bridge) was reduced as compared to the ligand alone (Fig.4(a)). This perhaps led to the occurrence of red shifted (25 nm) fluorescence emission band upon chelation of the ligand with

two Zn^{2+} ions in the proposed fashion. Selected orbitals and their corresponding energies for both $\mathbf{L_1}$ and its Zn complex were provided in supporting information (Table.S1 and S2 in supporting information) which might have been playing vital role in the optical spectral outcome.

Cellular Sensing of Zn^{2+}

Owing to the promising response of $\mathbf{L_1}$ towards Zn^{2+} and its intense emission in visible region, it was envisaged that compound $\mathbf{L_1}$ could be used for detection of intracellular Zn^{2+} by fluorescence-based imaging of live cells. However, to accomplish this target, it was imperative to initially evaluate the cytotoxic potential of compound $\mathbf{L_1}$ on live cells. The well-established MTT (3-(4,5-dimethylthiazol-2-yl)-2,5-diphenyltetrazolium bromide) assay, which is based on mitochondrial dehydrogenase activity of viable cells,

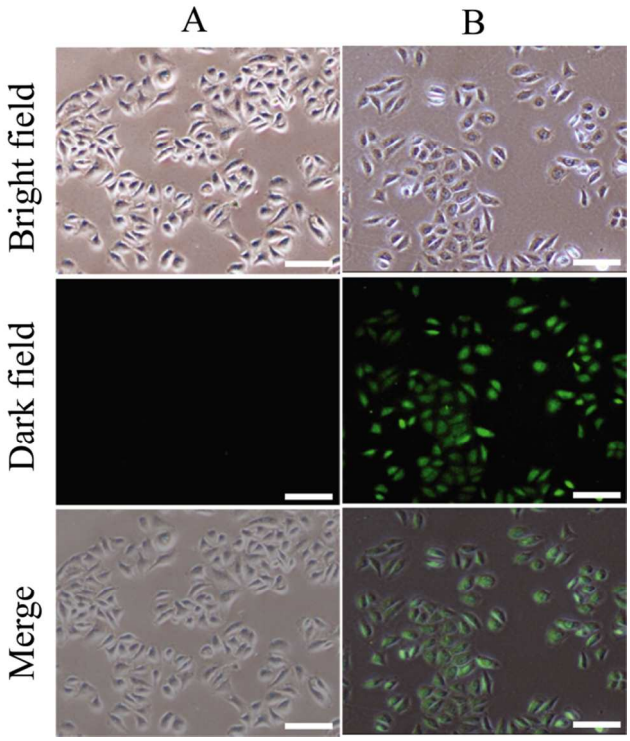

Fig. 5: Fluorescence microscopic images of HeLa cells after adding 25 μM of $\mathbf{L_1}$ (column A) and after subsequent treatment with 50 μM Zn^{2+} (Column B). Scale bar for the images is 100 μm.

illustrated that neither $\mathbf{L_1}$ nor its zinc complex was able to exhibit any effect on the viability of HeLa cells (human cervical carcinoma cells), even at concentrations as high as 50 μM (Fig. S15). The results obtained from the *in vitro* cytotoxic assay were encouraging and suggested that a ligand concentration upto 50 μM can perhaps be employed for the fluorescence imaging studies of $\mathbf{L_1}$ and $\mathbf{L_1}$–Zn complex in live cells. Hence, to evaluate the efficiency of compound $\mathbf{L_1}$ as a chemosensor for intracellular detection of Zn^{2+} by fluorescence microscopy, HeLa cells were treated with 25 μM $\mathbf{L_1}$ solution for 1 h followed by incubation with 50 μM $Zn(ClO_4)_2$ to promote the formation of $\mathbf{L_1}$–Zn complex. Fluorescence microscope analysis revealed that compound $\mathbf{L_1}$ alone failed to exhibit any fluorescence in HeLa cells (Fig. 5). However, when treated with $Zn(ClO_4)_2$, a distinct and strong turn-on green fluorescence was observed which could be attributed to the formation of intracellular $\mathbf{L_1}$-Zn complex. This observation is in well agreement with the results observed earlier in solution studies. It may be mentioned here that brightfield images of treated HeLa cells revealed the characteristic morphological attribute of HeLa cells, which also suggested that the cells were viable. The fluorescence microscopic analysis strongly suggested that compound $\mathbf{L_1}$ could readily traverse the membrane barrier, pervade into HeLa cells, and rapidly sense intracellular Zn^{2+}.

Conclusion

In brief, we have synthesized and demonstrated the sensing potential of an efficient receptor ($\mathbf{L_1}$) for Zn^{2+} in physiological condition (99.7% HEPPES buffer, pH=7.4). The ligand $\mathbf{L_1}$ can be excited in visible light and has high selectivity towards Zn^{2+} over other biologically significant metal ions, even in the presence of higher concentration of competing metal ions. The judicious choice of a DFMP core in the receptor rendered a strong CHEF-based turn-on fluorescence following chelation of Zn^{2+} by the hydroxide group and the Schiff base N-atoms. Theoretical calculations of $\mathbf{L_1}$ and $\mathbf{L_1}$-zn ensemble also support our proposed mechanism. Due to the high selectivity of $\mathbf{L_1}$ towards Zn^{2+} in exclusively physiological medium and non-cytotoxic nature, the newly developed receptor was successful in sensing intracellular Zn^{2+}, wherein immensely intense turn-on green fluorescence was manifested in HeLa cells. The non-cytotoxic behaviour of $\mathbf{L_1}$ and its capability of sensing intracellular Zn^{2+} are well for future *in vivo* biomedical applications of the sensor.

Acknowledgements

The authors acknowledge CSIR (01/2727/13/EMR-II), Science & Engineering Research Board (SR/S1/OC-62/2011) and Department of Biotechnology (BT/01/NE/PS/08), New Delhi, India for financial support and Central Instruments Facility, IIT Guwahati for providing instrument facilities. B.K.D, D.T, S.S and C.K acknowledge IIT Guwahati for research fellowship. Special thanks are due to Moumita Pait for her kind cooperation.

Notes and references

[a] Department of Chemistry, Indian Institute of Technology Guwahati, Guwahati 781039, India. Fax: + 91 361 2582349; Tel: +91 3612582313; E-mail: gdas@iitg.ernet.in

[b] Department of Biotechnology, Indian Institute of Technology Guwahati, Guwahati 781039, India. Fax: +91 361 2582249; Tel: +91 361 2582205; E-mail: aramesh@iitg.ernet.in

Electronic Supplementary Information (ESI) available: ^{1}H-NMR data, ^{13}C-NMR data, ESI-MS spectra, ^{1}H-NMR titration data, Benesi Hildebrand plot, Job's plot and tables of DFT calculations. See DOI: 10.1039/b000000x/

1 (a) P. N. Prasad, *Introduction to Biophotonics,* Wiley, NJ, 2003; (b) J. B. Pawley, *Handbook of Biological Confocal Microscopy,* Plenum, New York, 1995; (c) J. W. Lichtman and J.-A. Conchello, *Nat. Methods*, 2005, **2**, 910.

2 (a) B. L. Vallee and K. H. Falchuk, *Physiol. Rev.,* 1993, **73**, 79; (b) J. M. Berg and Y. Shi, *Science,* 1996, **271**, 1081; (c) T. V. O'Halloran, *Science,* 1993, **261**, 715; (d) C. J. Frederickson, J. Y. Koh and A. I. Bush, *Nat. Rev. Neurosci.,* 2005, **6**, 449; (e) P. J. Fraker and L. E. King, *Annu. Rev. Nutr.,* 2004, **24**, 277; (f) A. C. Burdette and S. J. Lippard, *Proc. Natl. Acad. Sci. U. S. A.,* 2003, **100**, 3605; (g) Z. C. Xu, J. Y. Yoon and D. R. Spring, *Chem. Soc. Rev.,* 2010, **39**, 1996.

3 (a) M. J. Hambidge, *Nutr.,* 2000, **130**, 1344S; (b) J. Y. Koh, S. W. Suh, B. J. Gwag, Y. Y. He, C. Y. Hsu and D. W. Choi, *Science,* 1996, **272**, 1013; (c) H. Bartlett and F. Eperjesi, *Ophthalmic Physiol. Opt.,* 2003, **23**, 383; (d) C. Sindreu, R. D. Palmiter and D. R. Storm, *Proc. Natl. Acad. Sci. U. S. A.,* 2011, **108**, 3366; (e) A. I. Bush, *Alzheimer Dis. Assoc. Disord.,* 2003, **17**, 147; (f) C. L. F. Walker, Z. A. Bhutta, N. Bhandari, T. Teka, F. Shahid, S. Taneja and R. E. Black, *Am. J. Clin. Nutr.,* 2007, **85**, 887.

4 A. Voegelin, S. Poster, A. C. Scheinost, M. A. Marcus and R. Kretzsch-mar, *Environ. Sci. Technol.*, 2005, **39**, 6616.

5 (a) E. Tomat and S. J. Lippard, *Curr. Opin. Chem. Biol.,* 2010, **14**, 225; (b) Z. Xu, J. Yoon and D. R. Spring, *Chem. Soc. Rev.,* 2010, **39**, 1996; (c) E. L. Que, D. W. Domaille and C. J. Chang, *Chem. Rev.,* 2008, **108**, 1517; (d) P. Jiang and Z. Guo, *Coord. Chem. Rev.,* 2004, **248**, 205.

6 (a) E. M. Nolan and S. J. Lippard, *J. Am. Chem. Soc.,* 2003, **125**, 14270; (b) S. Atilgan, T. Ozdemir and E. U. Akkaya, *Org. Lett.,* 2010, **12**, 4792; (c) J. L. Sessler and J. M. Davis, *Acc. Chem. Res.,* 2001, **34**, 989; (d) B. W. Michel, A. R. Lippert and C. J. Chang, *J. Am. Chem. Soc.,* 2012, **134**, 15668.

7 (a) H. Giloh and J. W. Sedat, *Science*, 1982, **217**, 1252; (b) D. Sinnecker, P. Voigt, N. Hellwig and M. Schaefer, *Biochemistry,* 2005, **44**, 7085; (c) J. N. Henderson, H.-W. Ai, R. E. Campbell and S. J. Remington, *Proc. Natl. Acad. Sci. U. S. A.*, 2007, **104**, 6672; (d) N. Periasamy, S. Bicknese and A. S. Verkman, *Photochem. Photobiol.,* 1996, **63**, 265.

8 (a) T. E. Kaiser, V. Stepanenko and F. Würthner, *J. Am. Chem. Soc.*, 2009, **131**, 6719; (b) K.-R. Wang, D.-S. Guo, B.-P. Jiang, Z.-H. Sun and Y. Liu, *J. Phys. Chem. B,* 2010, **114**, 101; (c) Q. Zhao, S. Zhang, Y. Liu, J. Mei, S. Chen, P. Lu, A. Qin, Y. Ma, J. Z. Sun and B. Z. Tang, *J. Mater. Chem.*, 2012, **22**, 7387.

9 (a) F. Qian, C. Zhang, Y. Zhang, W. He, X. Gao, P. Hu and Z. Guo, *J. Am. Chem. Soc.*, 2009, **131**, 1460; (b) T. Hirayama, K. Okuda and H. Nagasawa, *Chem. Sci.,* 2013, **4**, 1250; (c) Y. Qian, J. Karpus, O. Kabil, S.-Y. Zhang, H.-L. Zhu, R. Banerjee, J. Zhao and C. He, *Nat. Commun.*, 2011, **2**, 495; (d) H. S. Jung, P. S. Kwon, J. W. Lee, J. Kim, C. S. Hong, J. W. Kim, S. Yan, J. H. Lee, T. Joo and J. S. Kim, *J. Am. Chem. Soc.,* 2009, **131**, 2008.

10 (a) Z. Xu, Y. Xiao, X. Qian, J. Cui and D. Cui, *Org. Lett.,* 2005, **7**, 889; (b) J. B. Wang, X. F. Qian and J. N. Cui, *J. Org. Chem.*, 2006, **71**, 4308.

11 (a) T. Gunnlaugsson, A. P. Davis, J. E. O'Brien and M. Glynn, *Org. Lett.*, 2002, **4**, 2449; (b) D. H. Vance and A. W. Czarnik, *J. Am. Chem. Soc.*, 1994, **116**, 9397; (c) S. K. Kim and J. Yoon, *Chem. Commun.*, 2002, 770.

12 (a) N. C. Lim, J. V. Schuster, M. C. Porto, M. A. Tanudra, L. Yao, H. C. Freake and C. Bruckner, *Inorg. Chem.*, 2005, **44**, 2018; (b) S. Guha, S. Lohar, A. Banerjee, A. Sahana, A. Chaterjee, S. K. Mukherjee, J. S. Matalobos and D. Das, *Talanta,* 2012, **91**, 18; (c) S. Das, A. Sahana, A. Banerjee, S. Lohar, S. Guha, J. S. Matalobos and D. Das, *Anal. Methods*, 2012, **4**, 2254.

13 (a) P. D. Beer, *Acc. Chem. Res.,* 1998, **31**, 71; (b) M. J. Kim, R. Konduri, H. Ye, F. M. MacDonnell, F. Puntoriero, S. Serroni, S. Campagna, T. Holder, G. Kinsel and K. Rajeshwar, *Inorg. Chem.,* 2002, **41**, 2471.

14 (a) S. Nishizawa, Y. Kato and N. Teramae, *J. Am. Chem. Soc.,* 1999, **121**, 9463; (b) J.-S. Wu, J.-H. Zhou, P.-F. Wang, X.-H. Zhang and S.- K. Wu, *Org. Lett.,* 2005, **7**, 2133; (c) B. Schazmann, N. Alhashimy and D. Diamond, *J. Am. Chem. Soc.*, 2006, **128**, 8607; (d) A. Banerjee, A. Sahana, S. Guha, S. Lohar, I. Hauli, S. K. Mukhopadhyay, J. S. Matalobos and D. Das, *Inorg. Chem.*, 2012, **51**, 5699; (e) A. Sahana, A. Banerjee, S. Lohar, S. Guha, S. Das, S. K. Mukhopadhyay and D. Das, *Analyst,* 2012, **137**, 3910.

15 J.-S. Wu, W.-M. Liu, X.-Q. Zhuang, F. Wang, P.-F. Wang, S.-L. Tao, X.-H. Zhang, S.-K. Wu and S.-T. Lee, *Org. Lett.*, 2007, **9**, 33.

16 S. Lohar, A. Sahana, A. Banerjee, A. Banik, S. K. Mukhopadhyay, J. S. Matalobos and D. Das, *Anal. Chem.*, 2013, **85**, 1778.

17 X. Peng, Y. Wu, J. Fan, M. Tian and K. Han, *J. Org. Chem.*, 2005, **70**, 10524.

18 (a) S. Das, S. Guha, A. Banerjee, S. Lohar, A. Sahana and D. Das, *Org. Biomol. Chem.*, 2011, **9**, 7097.

19 (a) J. M. Serin, D. W. Brousmiche and J. M. J. Frechet, *J. Am. Chem. Soc.*, 2002, **124**, 11848; (b) A. E. Albers, V. S. Okreglak and C. J. Chang, *J. Am. Chem. Soc.*, 2006, **128**, 9640; (c) S. H. Lee, S. K. Kim, J. H. Bok, S. H. Lee, J. Yoon, K. Lee and J. S. Kim, *Tetrahedron Lett.*, 2005, **46**, 8163; (d) W. R. Dichtel, J. M. Serin, C. Edder, J. M. J. Frechet, M. Matuszewski, L.-S. Tan, T. Y. Ohulchanskyy and P. N. Prasad, *J. Am. Chem. Soc.,* 2004, **126**, 538; (e) M. Suresh, S. Mishra, S. K. Mishra, E. Suresh, A. K. Mandal, A. Shrivastav and A. Das, *Org. Lett.,* 2009, **11**, 2740; (f) P. Mahato, S. Saha, E. Suresh, R. D. Liddo, P. P. Parnigotto, M. T. Conconi, M. K. Kesharwani, B. Ganguly and A. Das, *Inorg. Chem.*, 2012, **51**, 1769; (g) K. Sreenath, J. Allen, R. M. W. Davidson and L. Zhu, *Chem. Commun.*, 2011, **47**, 11730; (h) R. J. Wandell, A. H. Younes, L. Zhu, *New J. Chem.*, 2010, **34**, 2176.

20 (a) X. Peng, T. Wu, J. Fan, J. Wang, S. Zhang, F. Song and S. Sun, *Angew. Chem., Int. Ed.,* 2011, **50**, 4180; (b) Z. Xu, J.

Yoon and D. R. Spring, *Chem. Soc. Rev.,* 2010, **39**, 1996; (c) Z.-Q. Guo, W.-H. Zhu, M.-M. Zhu, X.-M. Wu and H. Tian, *Chem. Eur. J.*, 2010, **16**, 14424; (d) Z.-P. Liu, C.-L. Zhang, Y.-L. Li, Z.-Y. Wu, F. Qian, X.-L. Yang, W.-J. He, X. Gao and Z.-J. Guo, *Org. Lett.*, 2009, **11**, 795; (e) C. E. Felton, L.P. Harding, J. E. Jones, B. M. Kariuki, S. J. A. Pope and C. R. Rice, *Chem. Commun.,* 2008, 6185; (f) H.-H. Wang, Q. Gan, X.-J. Wang, L. Xue, S.-H. Liu and H. Jiang, *Org. Lett.*, 2007, **9**, 4995.

21 (a) S. Maruyama, K. Kikuchi, T. Hirano, Y. Urano and T. Nagano, *J. Am. Chem. Soc.*, 2002, **124**, 10650; (b) K. Kiyose, H. Kojima, Y. Urano and T. Nagano, *J. Am. Chem. Soc.*, 2006, **128**, 6548; (c) C. C. Woodroofe and S. J. Lippard, *J. Am. Chem. Soc.,* 2003, **125**, 11458; (d) M. Taki, J. L. Wolford and T. V. O'Halloran, *J. Am. Chem. Soc.*, 2004, **126**, 712; (e) C. J. Chang, J. Jaworski, E. M. Nolan, M. Sheng and S. J. Lippard, *Proc. Natl. Acad. Sci. U.S.A.*, 2004, **101**, 1129; (f) M. M. Henary, Y. Wu and C. J. Fahrni, *Chem.−Eur. J.*, 2004, **10**, 3015; (g) N. C. Lim, C. Bruckner, *Chem. Commun.*, 2004, 1094. (h) A. Ajayaghosh, P. Carol and S. Sreejith, *J. Am. Chem. Soc.*, 2005, **127**, 14962; (i) K. Komatsu, Y. Urano, H. Kojima and T. Nagano, *J. Am. Chem. Soc.,* 2007, **129**, 13447; (j) X. Zhang, K. S. Lovejoy, A. Jasanoff and S. J. Lippard, *Proc. Natl. Acad. Sci. U.S.A.*, 2007, **104**, 10780.

22 (a) B. K. Datta, C. Kar, A. Basu and G. Das, *Tetrahedron Lett.,* 2013, **54**, 771; (b) S. K. Dey, and G. Das, *Chem. Commun.,* 2011, **47,** 4983; (c) C. Kar, A. Basu and G. Das, *Tetrahedron Lett.,* 2012, **53,** 4754; (d) A. Basu and G. Das, *Dalton Trans.,* 2011, **40,** 2837; (e) C. Kar, M. D. Adhikari, A. Ramesh and G. Das, *RSC Adv.,* 2012, **2,** 9201; (f) C. Kar and G. Das, *J. Photochem. Photobiol., A*., 2013, **251,** 128; (g) C. Kar, M. D. Adhikari, A. Ramesh and G. Das, *Inorg. Chem.,* 2013, **52,** 743; (h) B. K. Datta, S. Mukherjee, C. Kar, A. Ramesh and G. Das, *Anal. Chem.,* 2013, **85,** 8369; (i) C. Kar, M. D. Adhikari, B. K. Datta, A. Ramesh and G. Das, *Sens. Actuators, B,* 2013, **188,** 1132; (j) S. Samanta, S. Goswami, A. Ramesh and G. Das. *Sensor. Actuators, B,* 2013, **194**, 120.

23 D. A. Denton and H. Suschitzky, *J. Chem. Soc.*, 1963, 4741.

24 H. A. Benesi and J. H. Hildebrand, *J. Am. Chem. Soc.*, 1949, **71**, 2703.

